International Journal of Fluid Mechanics Research, Vol. 28, No. 4, 2001

Hydromagnetic Flow and Heat Transfer over a Non-Isothermal Power-Law Stretched Surface with Heat Generation[†]

Ali J. Chamkha
Department of Mechanical Engineering,
Kuwait University, Safat, 13060 Kuwait

General boundary-layer equations governing steady, laminar, hydromagnetic flow and heat transfer over a non-isothermal permeable surface stretching with a power-law velocity with heat generation and suction/injection effects and in the presence of a non-uniform transverse magnetic field are developed. A similarity transformation is used to transform the governing partial differential equations into ordinary differential equations. Linearized flow solutions for the case of large magnetic numbers are derived. The dimensionless similar equations are then solved numerically by using a standard fully implicit, iterative, tri-diagonal finite-difference method. Favorable agreement between the finite-difference and the linearized flow solutions are obtained. In addition, comparisons with previously published work on various aspects of the problem are performed and found to be in excellent agreement. A parametric study of all the physical parameters involved in the problem is conducted. A representative set of numerical results is illustrated graphically and discussed.

* * *

Introduction

There have been considerable work done on boundary-layer flow and heat transfer in a quiescent fluid driven by a stretched surface moving with a constant or variable velocity. This is due to many metallurgical and engineeirng applications such as hot rolling, metal and polymer sheet extrusion, drawing, annealing and tinning of copper wires, crystal growth, glass fiber production, paper production, and many others. The first to consider flow and heat transfer over a continuously moving surface with a uniform velocity was Sakiadis (1961 a, b) [22,23]. In later studies, Erickson et al. (1966) [15], Tsuo et al. (1967) [27], Fox et al. (1968) [16], Chen and Strobel (1980) [11], and Jacobi (1993) [19] verified and extended the works of Sakiadis (1961 a, b) [22,23]. It is worthy to mention that Jacobi (1993) [19] confirmed the flow field obtained by Sakiadis (1961 a, b) [22,23] for a uniform motion of the stretched surface.

There has also been research dealing with the problem of a stretched surface moving with a

[†] Received 29.06.2000

ISSN 1064-2277

linear velocity and various thermal boundary conditions (see, or instance, Crane (1970) [14], Gupta and Gupta (1977) [18], Vleggar (1977) [30], Soundalgekar and Murty (1980) [25], Grubka and Bobba (1985) [17] and Chen and Char (1988) [10]). Very recently, many investigations studying the consequent flow and heat transfer characteristics that are brought about by the movement of a stretched permeable and impermeable, isothermal and non-isothermal surface with a power-law velocity variation. Examples of these works are those of Banks (1983) [5] who considered the case of impermeable wall, and Ali (1994, 1995, 1996) [2–4] who presented various extensions to Banks' (1983) [5] problem in terms of flow and thermal boundary conditions.

There has been renewed interest in studying hydromagnetic flow and heat transfer of continuously stretched surfaces in the presence of a transverse magnetic field. This is because hydromagnetic flow and heat transfer have become more important industrially. For example, many metallurgical processes such as drawing, annealing and tinning of copper wires involve cooling of continuous strips or filaments by drawing them through a quiescent fluid. Controlling the rate of cooling in these processes can affect the properties of the final product. This can be done by using an electrically-conducting fluid and applying a magnetic field. Another application of hydromagnetics to metallurgy lies in the purification of molten metals from non-metallic inclusions (Vajravelu and Hadjinicolaou (1997) [28]). Cobble (1977) [13] obtained similarity solutions for hydromagnetic flow over a semi-infinite plate with suction and injection at the wall. Soundalgekar and Murty (1980) [25] had considered the thermal problem of Cobble (1977) [13]. Recently, Chandran et al. (1996) [9] made extensions to the above works and considered flow of an electrically-conducting fluid over a semi-infinite plate with suction and injection. Chakrabarti and Gupta (1979) [7] obtained a closed-form similarity solution for the problem of hydromagnetic flow of a linearly stretching surface in the presence of a constant transverse magnetic field. Chiam (1995) [12] extended the work of Chakrabarti and Gupta (1979) [7] to power-law velocity of the stretched surface. In Chiam's (1995) [12] problem, the magnetic field was assumed non-uniform so as to allow for similarity solution.

In certain industrial problems dealing with chemical reactions and dissociating fluids, heat generation/absorption effects become important (see Vajravelu and Nayfeh (1992) [29]). Moalem (1976) [21] considered temperature-dependent heat sources occurring in electrical heating. Other works dealing with heat generation effects can be found in the papers by Sparrow and Cess (1961) [26], Chamkha (1996) [8], and Vajravelu and Hadjinicolaou (1997) [28].

The present paper generalizes the works of both Chiam (1995) [12] and Ali (1995) [3] to include the influences of heat generation/absorption, non-uniform transverse magnetic field, and fluid suction or injection at the stretched surface.

Mathematical Formulation

Consider steady, laminar, hydromagnetic, two-dimensional boundary-layer flow and heat transfer in a quiescent electrically-conducting fluid driven by a non-isothermal permeable surface stretched by a power-law velocity and has a power-law temperature distribution with its axial or tangential distance. Fluid suction or injection is imposed at the boundary of the surface and a non-uniform transverse magnetic field is applied normal to the flow direction. The working fluid is assumed to be incompressible, viscous, heat generating or absorbing, electrically conducting and has constant properties. The magnetic Reynolds number is assumed to be small so that the induced magnetic field can be neglected. In addition, no external electric field is assumed to exist and the electric field due to the effect of charge polarization and the Hall effect of magnetohydrodynamics are neglected. The effects of viscous dissipation and Joule heating are also neglected. The basic equations for this

investigation can be written as (see Chiam (1995) [12], and Ali (1995) [3]):

$$\frac{\partial u}{\partial x} + \frac{\partial v}{\partial y} = 0, \tag{1}$$

$$u\frac{\partial u}{\partial x} + v\frac{\partial u}{\partial y} = \nu\frac{\partial^2 u}{\partial y^2} - \frac{\sigma B(x)^2}{\rho}\,u, \tag{2}$$

$$u\frac{\partial T}{\partial x} + v\frac{\partial T}{\partial y} = \alpha\frac{\partial^2 T}{\partial y^2} + \frac{Q(x)}{\rho c_p}\,(T - T_\infty), \tag{3}$$

where x and y are the axial or tangential and normal distances, respectively; u, v, T and T_∞ are the fluid x-component and y-component of velocity, temperature and the ambient temperature, respectively; ρ, ν, c_p and α are the fluid density, kinematic viscosity, specific heat at constant pressure and thermal diffusivity, respectively; σ, $B(x)$ and $Q(x)$ are the electrical conductivity, the variable magnetic induction and the heat generation/absorption coefficient, respectively. It should be mentioned that positive values of $Q(x)$ mean heat generation (source) and negative values of $Q(x)$ indicate heat absorption (sink). Also, it is noticed that the heat generation or absorption term is assumed to be dependent on the difference between the boundary-layer temperature and that of the free stream. This has been employed previously by Vajravelu and Hadjinicolaou (1997) [28] and is appropriate for boundary-layer applications in which this difference is significant.

The boundary conditions for this problem are:

$$\begin{gathered} u(x,0) = U_0 x^m,\ v(x,0) = v_w(x),\ T(x,0) = T_w(x) = Cx^n + T_\infty, \\ u(x,\infty) = 0,\ T(x,\infty) = T_\infty, \end{gathered} \tag{4}$$

where U_0, C, m and n are constants and $v_w(x)$ and $T_w(x)$ are the variable normal velocity and temperature at the wall, respectively. It should be noted that positive values of $v_w(x)$ correspond to fluid blowing or injection at the surface while negative values of $v_w(x)$ indicate fluid suction at the boundary.

Following Ali (1995) [3], Chiam (1995) [12] and Afzal (1993) [1], the following similarity transformation can be employed:

$$\begin{gathered} \eta(x,y) = y\sqrt{\frac{(m+1)U_0\,x^m}{2\nu x}}, \quad \psi(x,y) = F(\eta)\sqrt{\frac{2\,\nu\,U_0\,x^{m+1}}{m+1}}, \\ T(x,y) = Cx^n\theta(\eta) + T_\infty, \quad u = \frac{\partial\psi}{\partial y} = U_0 x^m F'(\eta), \\ v = -\frac{\partial\psi}{\partial x} = -\sqrt{\frac{2\,\nu\,U_0\,x^{m-1}}{m+1}}\left(\frac{m+1}{2}F(\eta) + \frac{m-1}{2}\,\eta\,F'(\eta)\right), \end{gathered} \tag{5}$$

where η, $F'(\eta)$ and $\theta(\eta)$ are the similarity variable, dimensionless velocity, and dimensionless temperature, respectively. Here, a prime denotes ordinary differentiation with respect to η. It can easily be verified that the balance of mass given by Eq. (1) is identically satisfied. A similarity solution arises if the magnetic induction $B(x)$ and the heat generation/absorption $Q(x)$ take on the forms

$$B(x) = B_0\,x^{(m-1)/2}, \quad Q(x) = Q_0\,x^{(m-1)}, \tag{6}$$

where B_0 and Q_0 are constants. Substitution of Eqs. (5) and (6) into Eqs. (2) and (3) and rearranging yields:

$$F''' + FF'' - \beta(F')^2 - \frac{\beta}{m}\,\mathrm{Ha}^2 F' = 0, \tag{7}$$

$$\theta'' + \mathrm{Pr}\,(F\theta' - \frac{\beta}{m}(nF' - \phi)\,\theta) = 0, \tag{8}$$

where

$$\beta = \frac{2m}{m+1}, \quad \mathrm{Ha}^2 = \frac{\sigma B_0^2}{\rho\, U_0}, \quad \mathrm{Pr} = \frac{\nu}{\alpha}, \quad \phi = \frac{Q_0}{\rho\, c_p U_0}. \tag{9}$$

Here, Ha is the Hartmann number; Pr is the Prandtl number and ϕ is the dimensionless heat generation/absorption coefficient which indicates heat generation for positive values and heat absorption for negative values.

The transformed boundary conditions become:

$$F'(0) = 1,\ F(0) = f_w\sqrt{\frac{2}{m+1}},\ \theta(0) = 0,\ F'(\infty) = 0,\ \theta(\infty) = 0, \tag{10}$$

where $f_w = v_w\sqrt{x^{1-m}/U_0\nu}$ is the dimensionless suction ($f_w < 0$) or injection ($f_w > 0$) velocity. It should be mentioned that if Ha and ϕ are formally set to zero, the equations reported by Ali (1995) [3] will be recovered. Also, if ϕ and f_w are equated to zero, then the flow equation given by Chiam (1995) [12] will result.

Of special interest and significance for this flow and heat transfer situation are the skin-friction coefficient and the Nusselt number. These are defined as follows:

$$\begin{aligned} C_f &= \frac{-\rho\,\nu\,\partial u/\partial y(x,0)}{\rho\, U_0\, x^m} = -\sqrt{\frac{m+1}{2}}\,\mathrm{Re}^{-1/2}F''(0), \\ \mathrm{Nu} &= \frac{-k\,\partial T/\partial y(x,0)}{k\,(T_w - T_\infty)/\nu} = -\sqrt{\frac{m+1}{2}}\,\mathrm{Re}^{-1/2}\theta'(0), \end{aligned} \tag{11}$$

where k is the fluid thermal conductivity and $\mathrm{Re} = U_0 x^{m+1}/\nu$ is the local Reynolds number.

For a linear surface velocity ($m = 1$), the flow similarity (7) and the corresponding boundary condition (10) require that both the applied magnetic field and the wall mass transfer to be uniform. For this case Chakrabarti and Gupta (1979) [7] have shown that the solution of Eq. (7) subject to the corresponding boundary conditions for F in Eq. (10) can be written as

$$F(\eta) = \alpha_1 + \alpha_2 \exp\,(-\alpha_3\eta), \tag{12}$$

where α_1, α_2 and α_3 are constants given by

$$\alpha_1 = \frac{1}{2(1+\mathrm{Ha}^2)}[-(1+2\mathrm{Ha}^2)f_w + (f_w^2 + 4(1+\mathrm{Ha}^2))^{1/2}], \tag{13}$$

$$\alpha_2 = \frac{2}{f_w - [f_w^2 + 4(1+\mathrm{Ha}^2)]^{1/2}}, \quad \alpha_3 = \frac{1}{2}[\alpha_1 + (\alpha_1^2 + 4\mathrm{Ha}^2)^{1/2}]. \tag{14}$$

The skin-friction coefficient for this case becomes

$$C_f = -\mathrm{Re}^{-1/2}\alpha_2\,\alpha_3^2, \tag{15}$$

where $\mathrm{Re} = U_0 x^2/\nu$ is the local Reynolds number for this case.

Approximate Closed-Form Solutions

It is obvious from Eqs. (7) and (8) that the flow problem is uncoupled from the thermal problem. Therefore, Eq. (7) can be solved independently of Eq. (8). An approximate linearized solution of Eq. (7) can be obtained for large Hartmann numbers. The procedure to be followed below is outlined by Chiam (1995) [12]. Let

$$z = \sqrt{\frac{\beta}{m}}\,\mathrm{Ha}\,\eta, \quad f(z) = \sqrt{\frac{\beta}{m}}\,\mathrm{Ha}\,f(\eta). \tag{16}$$

Substituting Eq. (12) into Eq. (7) gives:

$$f''' - f' = \varepsilon\,(\beta(f')^2 - ff''), \tag{17}$$

where $\varepsilon = m/(\beta \mathrm{Ha}^2)$. The corresponding boundary conditions become

$$f(0) = -f_s, \quad f'(0) = 1, \quad f'(\infty) = 0, \tag{18}$$

where $f_s = \mathrm{Ha} f_w \beta/m$. Using the series expansion method for small values of ε by assuming:

$$f(z) = f_0(z) + \varepsilon f_1(z) + \varepsilon^2 f_2(z) + \ldots \tag{19}$$

and substituting this into Eq. (17) and Eq. (18) result in the following set of equations and boundary conditions:

$$f_0''' - f_0' = 0, \tag{20}$$

$$f_1''' - f_1' = \beta(f_0')^2 - f_0 f_0'', \tag{21}$$

$$f_2''' - f_2' = 2\beta f_0' f_1' - f_0 f_1'' - f_0'' f_1, \tag{22}$$

$$f_0(0) = -f_s, \quad f_0'(0) = 1, \quad f_0'(\infty) = 0, \tag{23}$$

$$f_1(0) = 0, \quad f_1'(0) = 0, \quad f_1'(\infty) = 0, \tag{24}$$

$$f_2(0) = 0, \quad f_2'(0) = 0, \quad f_2'(\infty) = 0. \tag{25}$$

Without going into detail, it can be shown that

$$f_0(0) = 1 - f_s - \exp(-z), \tag{26}$$

$$\begin{aligned} f_1(z) &= -\frac{1}{6}(2 - 3f_s + \beta) + \frac{1}{6}(1 - 3f_s + 2\beta + (3 - 3f_s)z)\exp(-z) \\ &\quad + \frac{1}{6}(1 - \beta)\exp(-2z), \end{aligned} \tag{27}$$

$$\begin{aligned} f_2(z) &= \frac{1}{144}(8\beta^2 + 26\beta - 28\beta f_s - 44 f_s + 18 f_s^2 + 20) \\ &\quad + \frac{1}{144}(-20\beta^2 - 31\beta + 56\beta f_s + 16 f_s - 18 f_s^2 - 3 \\ &\quad + (-36\beta + 24\beta f_s + 48 f_s - 18 f_s^2 - 18)z) + (36 f_s - 18 f_s^2 - 18)z^2)\exp(-z) \\ &\quad + \frac{1}{36}(4\beta^2 - \beta - 7\beta f_s + 7 f_s + (6\beta - 6\beta f_s + 6 f_s - 6)z)\exp(-2z) \\ &\quad + \frac{1}{144}(-4\beta^2 + 9\beta - 5)\exp(-3z). \end{aligned} \tag{28}$$

The approximate solution for the skin-friction coefficient can then be predicted for this case from the following expression:

$$\begin{aligned} C_f &= -\sqrt{\frac{(m+1)\,\beta^3\,\mathrm{Ha}^6}{2m^2}}\,\mathrm{Re}^{-1/2} f''(0) \\ &= -\sqrt{\frac{(m+1)\,\beta^3\,\mathrm{Ha}^6}{2m^2}}\,\mathrm{Re}^{-1/2}(-1+\frac{\varepsilon}{6}\,(3f_s-2\beta-1) \\ &\quad +\frac{\varepsilon^2}{144}\,(8\beta^2+10\beta-8\beta f_s+8f_s-18f_s^2)) \end{aligned} \tag{29}$$

to second order in the small parameter ε. It should be mentioned that for $f_s = 0$ (impermeable surface) the approximate solutions reported in Eq. (26) through Eq. (28) and the expression for $f''(0)$ included in the definition of C_f in Eq. (29) are consistent with those reported by Chiam (1995) [12] for $f_s = 0$.

Numerical Method and Validation

The flow and heat transfer situation on a stretching sheet represented by Eq. (7) through Eq. (10) are nonlinear and, therefore, must be solved numerically. Both the fourth-order Runge Kutta method and the standard implicit finite-difference method discussed by Blottner (1970) [6] are appropriate numerical methods and often used in the solution of such equations because of their simplicity and ease of use. In the present work, the latter numerical method is chosen and employed in obtaining the graphical results to be presented subsequently.

Eqs. (7) and (8) are discretized using three-point central difference formulae with F' replaced by another variable V. The η direction is divided into 196 nodal points and a variable step size is used to account for the sharp changes in the variables in the region close to the plate surface where viscous effects dominate. The initial step size used is $\Delta\eta_1 = 0.001$ and the growth factor $K = 1.03$ such that $\Delta\eta_n = K\Delta\eta_{n-1}$ (where the subscript n is the number of nodes minus one). The ordinary differential equations are then converted into linear algebraic equations that are solved by the Thomas algorithm discussed by Blottner (1970) [6]. Iteration is employed to deal with the nonlinear nature of the governing equations. The convergence criterion employed in this work was based on the relative difference between the current and the previous iterations. When this difference or error reached 10^{-5}, then the solution was assumed converged and the iteration process was terminated. More details of the numerical solution and the procedure followed can be explained as follows:

Consider Eq. (7) governing the dimensionless function F. By defining

$$V = F'. \tag{30}$$

Eq. (7) may be written (before the central-difference formulae are used) as:

$$\pi_1 V'' + \pi_2 V' + \pi_3 V + \pi_4 = 0, \tag{31}$$

where

$$\pi_1 = 1, \quad \pi_2 = F, \quad \pi_3 = -M - \beta V, \quad \pi_4 = 0, \quad M = \frac{\beta}{m}\,\mathrm{Ha}^2. \tag{32}$$

Similarly, Eq. (8) can be written as:

$$\pi_1\theta'' + \pi_2\theta' + \pi_3\theta + \pi_4 = 0, \tag{33}$$

where

$$\pi_1 = 1, \quad \pi_2 = \mathrm{Pr}\, F, \quad \pi_3 = -\mathrm{Pr}\,\frac{\beta}{m}\,(nV - \phi), \quad \pi_4 = 0. \tag{34}$$

The boundary conditions for V and θ are:

$$V(0) = 0, \quad V(\eta_{\max}) = 0, \quad \theta(0) = 1, \quad \theta(\eta_{\max}) = 0, \tag{35}$$

where infinity is replaced by $\eta_{\max}$ which is set to a maximum value of 20 in the present work. It should be reminded that the relation between the fluid tangential velocity u and the function V is given in Eq. (5). In the discussion of the numerical results to be reported subsequently, V is called the fluid velocity. This is done merely to give significance to this function as a flow property.

The coefficients π_1, π_2, π_3 and π_4 in the inner iteration step of each of Eqs. (31) and (33) are evaluated using the solution from the previous iteration step. Eq. (31) and Eq. (33) are then converted into tri-diagonal finite-difference algebraic equations of the form:

$$A_n G_{n-1} + B_n G_n + C_n G_{n+1} = D_n, \tag{36}$$

where G stands for V or θ and A_n, B_n, C_n and D_n are related to the π's and the step sizes used (see, Blottner, 1970 [6]). These resulting equations are then solved using the Thomas' algorithm.

Eq. (30) can be integrated by the trapezoidal rule to give:

$$F_{n+1} = F_n + \frac{(V_{n+1} + V_n)\,\Delta\eta_n}{2}, \tag{37}$$

where n corresponds to the n^{th} point along the η direction and the boundary condition for F at $\eta = 0$ is:

$$F(0) = -f_w \frac{2}{m+1}, \tag{38}$$

Table 1 presents a comparison between $F''(0)$ (which is directly proportional to the skin-friction coefficient) obtained from the approximate closed-form solutions given by Eq. (26) through Eq. (29) for large values of M and that obtained numerically by the finite-difference method.

It is clearly seen from this table that, for the various values of f_w, m, and M, these results are in excellent agreement. This is an evidence that the numerical results are accurate.

Table 2 shows a comparison between the numerical results of $F''(0)$ for the case of impermeable surface ($f_w = 0$) reported by Chiam (1995) [12] and the numerical results obtained in the present work. As is evident from these solutions, they are in excellent agreement. This provides another separate comparison for the hydrodynamic problem with previously published work.

Table 3 and Table 4 report comparisons of the Nusselt number $\mathrm{Nu}\,\mathrm{Re}^{-1/2}$ and heat flux $\theta'(0)$ with various previously published results for the uniformly-accelerated and linearly-accelerated isothermal surface, respectively. It is clear from these tables that the present predicted results for $\mathrm{Nu}\,\mathrm{Re}^{-1/2}$ agree well with those reported by previous investigators.

Finally, Table 5 gives a comparison of the Nusselt number for various wall suction and injection, accelerated and decelerated, and isothermal and non-isothermal surface conditions to those reported by Ali (1995) [3]. The excellent agreement shown between these results lends more confidence to the accuracy of the numerical procedure.

Results and Discussion

Many numerical results were obtained throughout the course of this work. A representative set of these results is shown graphically in Fig. 1 through 16 to illustrate special features for the hydrodynamic and thermal characteristics of the problem.

Fig. 1 and Fig. 2 present representative velocity (V) and temperature θ profiles for hydromagnetic flow and heat transfer over an impermeable ($f_w = 0$) surface for various power-law stretching velocity conditions, respectively. Increases in the wall stretching velocity exponent m have a tendency to reduce the fluid velocity and to increase its temperature. This is depicted in the respective decreases in V and increases in θ as m increases in Fig. 1 and Fig. 2.

Fig. 3 and Fig. 4 show typical profiles for V and θ for impermeable plate and a fixed value of m for various values of the magnetic number M, respectively. Application of a transverse magnetic field normal to the flow direction gives rise to a resistive force called the Lorentz force. This force has the effect of slowing the motion of the fluid along the stretched surface and increasing its temperature. In addition, increasing the strength of the magnetic field further produces more reductions and increases in the fluid velocity and temperature, respectively. These characteristics are clearly shown in Fig. 3 and Fig. 4.

Fig. 5 and Fig. 6 illustrate the influence of fluid suction or injection at the plate surface on both the fluid velocity and temperature, respectively. As expected, imposition of fluid suction at the wall reduces both the hydrodynamic and thermal boundary layers close to the wall and, therefore, the fluid velocity and temperature along the surface or plate. On the other hand, injection of fluid at the wall produces the opposite effect, namely increased hydrodynamic and thermal boundary layers and enhanced velocity and temperature fields. These behaviors are clearly illustrated by the increases in the profiles of both V and θ as the suction/injection coefficient f_w increases as shown in Fig. 5 and Fig. 6. The reader is reminded again that negative values of f_w indicate suction and positive values of f_w, correspond to injection or blowing.

Fig. 7 through Fig. 9 depict the influence of the Prandtl number Pr, the wall temperature exponent n, and the heat generation/absorption coefficient ϕ on the temperature profiles θ, respectively. As expected, increases in either of the Prandtl number Pr or the wall temperature exponent n produce reductions in the thermal boundary layer, thus, reducing the fluid temperature. In addition, as the heat generation/absorption coefficient ϕ increases, the fluid temperature increases. It should be noted that for large heat generation effects ($\phi = 0.2$) a distinctive peak in the temperature profile occurs above the wall. This is in constrast with the cases of smaller heat generation effects ($\phi < 0.1$) in which the maximum temperature occurs at the wall. These facts are clearly shown in Fig. 7 through Fig. 9.

Fig. 10 and Fig. 11 illustrate the influence of both of the magnetic number M, the wall stretching velocity exponent m and the suction/injection coefficient f_w, on the skin-friction coefficient, respectively. As mentioned before, increases in either M or m cause decreases in the velocity profiles V and the boundary-layer thickness. This causes the slope of V at the wall to increase which results in increasing the skin-friction coefficient C_f. However, as f_w, increases, V increases while its slope at the wall decreases. This results in reductions in C_f. These characteristics are evident from the increases in C_f as either M or m increases and decreases in C_f as f_w increases shown in Fig. 10 and Fig. 11.

Fig. 12 through Fig. 14 show the effects of the Prandtl number Pr, the wall stretching velocity exponent m, the magnetic number M, and the suction/injection coefficient f_w on the Nusselt number Nu, respectively. Again, as Pr increases, the thermal boundary layer decreases. This causes the

Table 1
Comparison of $F''(0)$ for various values of f_w, m and M

f_w	m	M	$F''(0)$ approximate	$F''(0)$ finite-difference
0	-0.5	100	-9.97992	-9.95156
0	0	100	-10.01843	-10.01667
0	1.0	100	-10.04988	-10.05176
0	3.0	100	-10.06644	-10.06857
0.1	-0.5	100	-9.85008	-9.90123
0.1	0	100	-9.94613	-9.96820
0.1	1.0	100	-10.00000	-10.00159
0.1	3.0	100	-10.03117	-10.01831
-0.1	-0.5	100	-10.05075	-10.00174
-0.1	0	100	-10.08771	-10.06873
-0.1	1.0	100	-10.10000	-10.10153
-0.1	3.0	100	-10.10184	-10.11856
0.2	3.0	5	-2.44490	-2.42069
0.2	3.0	10	-3.29632	-3.27005
0.2	3.0	50	-7.09442	-7.06680
0.2	3.0	100	-9.99602	-9.96863

Table 2
Comparison of $F''(0)$ for $f_w = 0$ and various values of M with Chiam (1995) [12]

β	M	Chiam (1995) [12]	Present results
1.5	0	-1.14860	-1.14993
5.0	0	-1.90253	-1.90590
-1.0	0	0.00000	-2.197E-3
-1.5	0	0.72725	0.72339
1.5	1	-1.52527	-1.52683
1.5	5	-2.51615	-2.51797
1.5	10	-3.36631	-3.36834
1.5	100	-10.0664	-10.06857
-1.0	1	-0.85111	-0.85165
-1.0	5	-2.16287	-2.16409
-1.0	10	-3.11003	-3.11108
-1.0	100	-9.98335	-9.98501

Table 3
Comparison of $\mathrm{Nu}\,\mathrm{Re}^{1/2}$ for various Prandtl numbers to previously published data
$m = 0, n = 0, f_w = 0, M = 0, \phi = 0$

Pr	Jacobi (1993) [19]	Soundalgekar and Murty (1980) [24]	Chen and Strobel (1980) [11]	Tsou et al. (1967) [27]	Ali (1995) [3]	Present results
0.7	0.3492	0.3508	0.34924	0.3492	0.3476	0.3524
1.0	0.4438	—	—	0.4438	0.4416	0.4453
10.0	1.6790	1.6808	—	1.6804	1.6713	1.6830

Table 4
Comparison of $\theta'(0)$ for various Prandtl numbers to previously published data
$m = 1, n = 1, M = 0, \phi = 0$

f_w	Pr	Grubka and Bobba (1985) [17]	Lakshmisha et al. (1988) [20]	Gupta and Gupta (1977) [18]	Ali (1995) [3]	Present results
0	0.7	—	-0.45446	—	-0.45255	-0.45584
0	1.0	-0.5820	—	-0.5820	-0.59988	-0.58331
0	10.0	-2.3080	—	—	-2.29589	-2.31009
1.067	1.0	—	—	-0.1105	-0.10996	-0.11288

Table 5
Comparison of $\mathrm{Nu}\,\mathrm{Re}^{-1/2}$ for various f_w, m, n
and Pr values for $M = 0$, $\phi = 0$ with Ali (1995) [3]

f_w	m	n	Pr	Ali (1995) [3]	Present results
-0.1	-0.2	-1.0	0.72	-0.82805	-0.80783
0.0	-0.2	-1.0	0.72	-1.23829	-1.20560
0.1	-0.2	-1.0	0.72	-2.00360	-1.93653
0.2	-0.2	-1.0	0.72	-4.26117	-4.02700
0.2	1.0	-1.0	0.72	-0.14345	-0.14084
0,2	5.0	-1.0	0.72	0.43605	0.44051
-0.2	1.0	-1.0	0.72	0.14103	0.14611
-0.2	1.0	0.0	0.72	0.55360	0.55795
-0.2	1.0	1.0	0.72	0.87585	0.88128
0.0	5.0	1.0	0.72	0.97497	0.98107
0.0	5.0	1.0	1.0	1.22255	1.22879
0.0	5.0	1.0	3.0	2.43543	2.44795
0.0	5.0	1.0	10.0	4.81930	4.84620

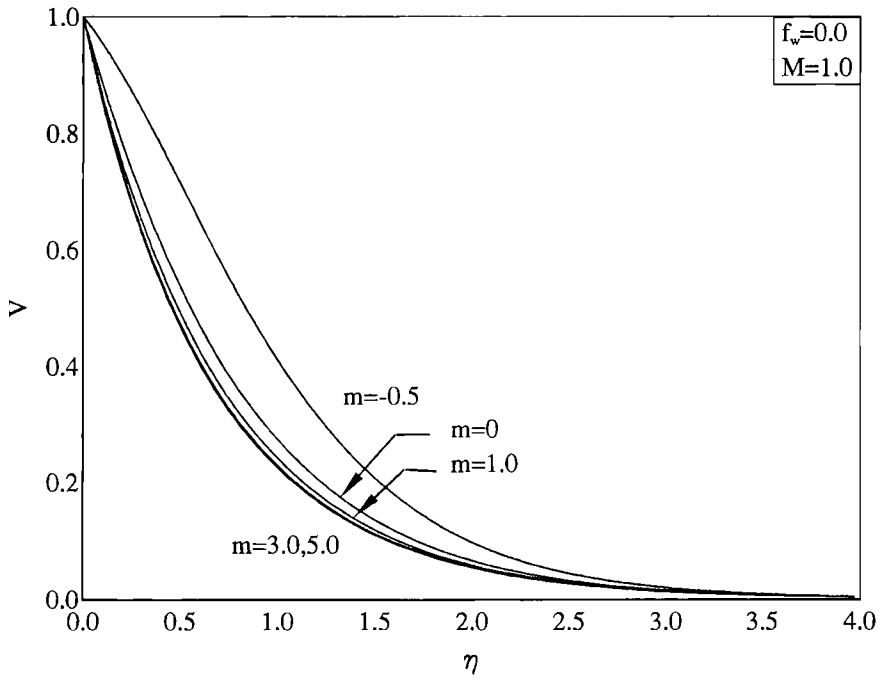

Fig. 1. Effects of m on velocity profiles.

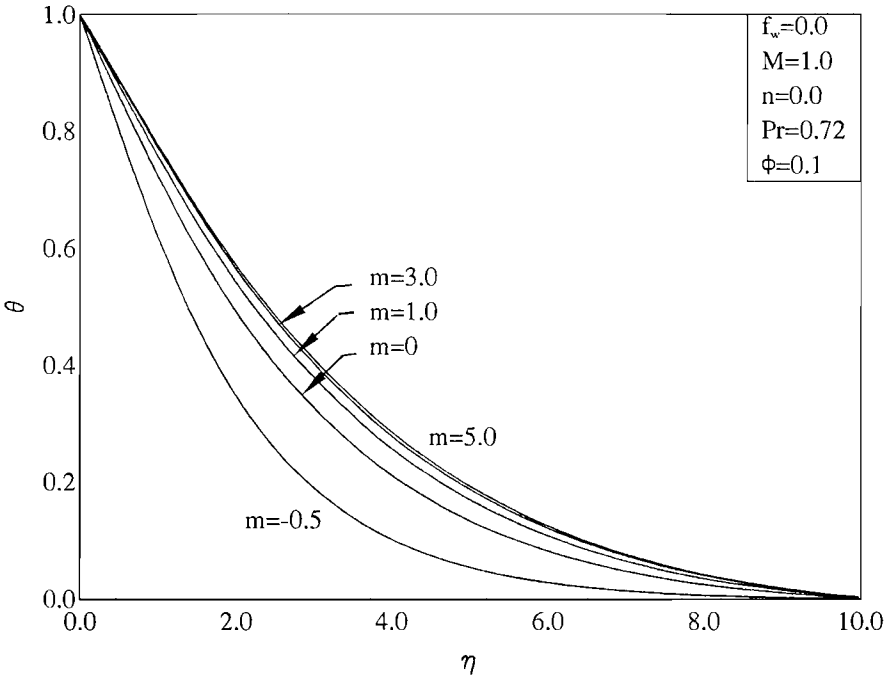

Fig. 2. Effects of m on temperature profiles.

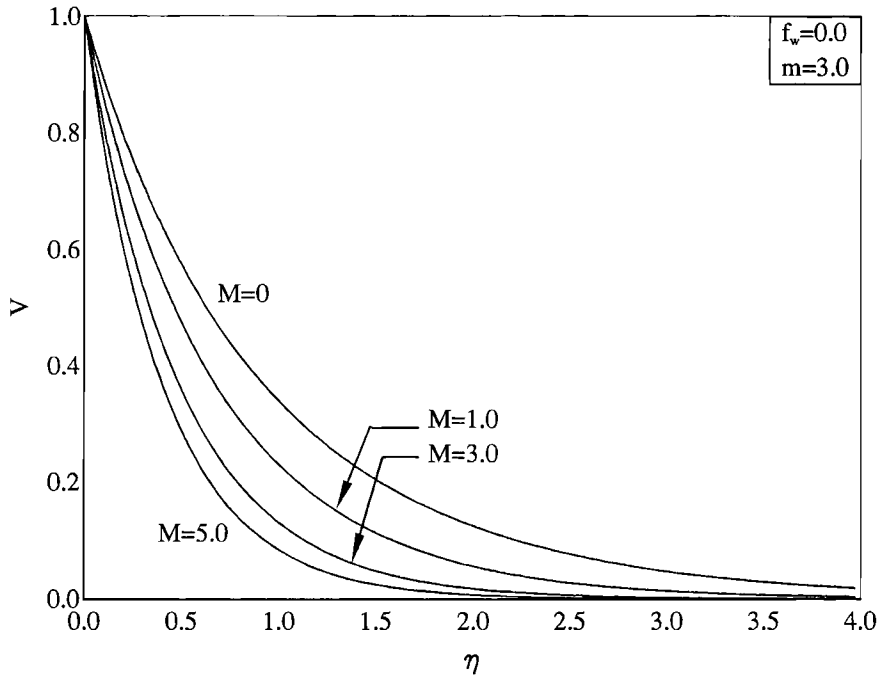

Fig. 3. Effects of M on velocity profiles.

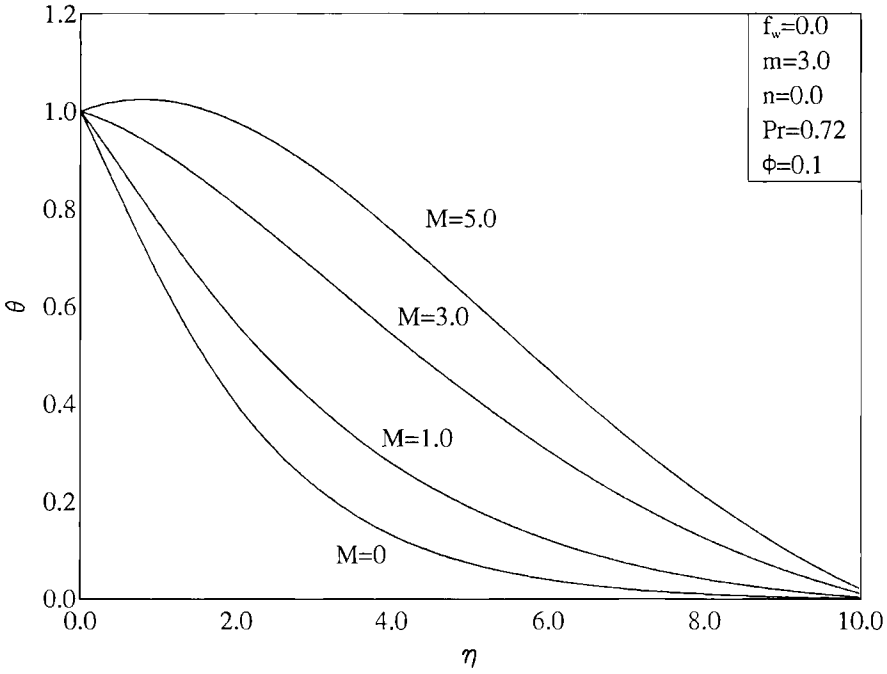

Fig. 4. Effects of M on temperature profiles.

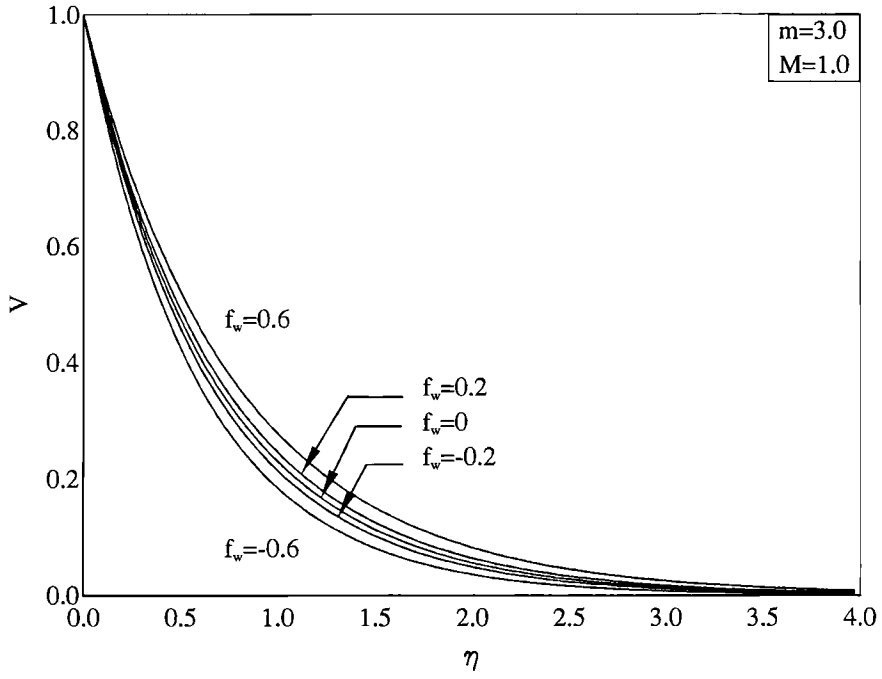

Fig. 5. Effects of f_w on velocity profiles.

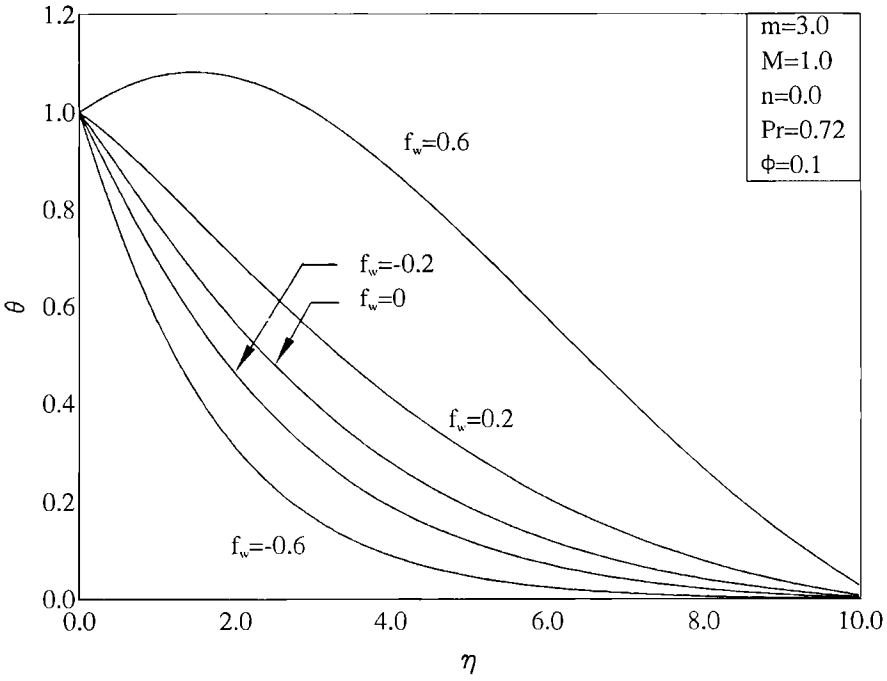

Fig. 6. Effects of f_w on temperature profiles.

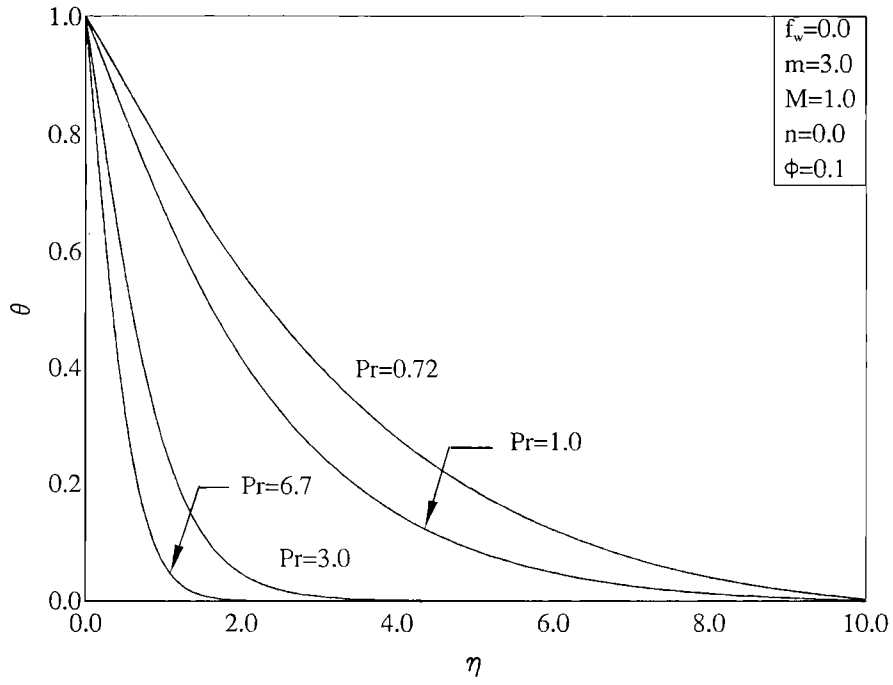

Fig. 7. Effects of Pr on temperature profiles.

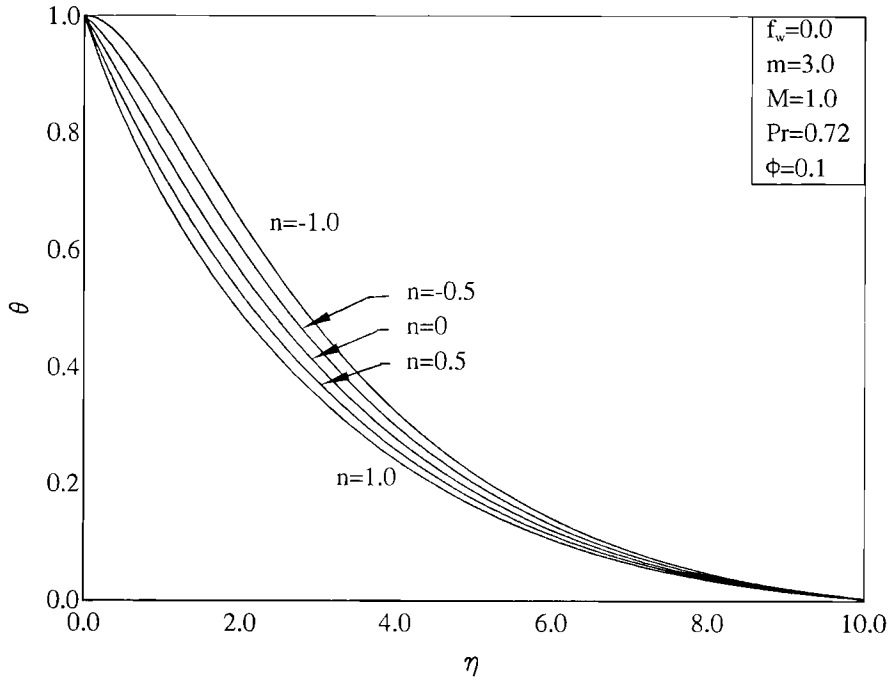

Fig. 8. Effects of n on temperature profiles.

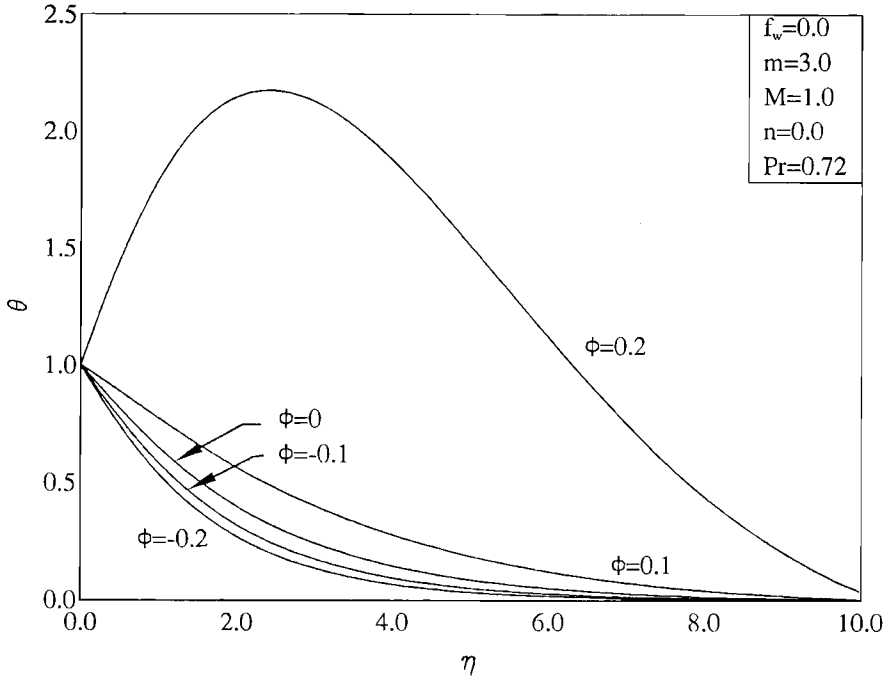

Fig. 9. Effects of ϕ on temperature profiles.

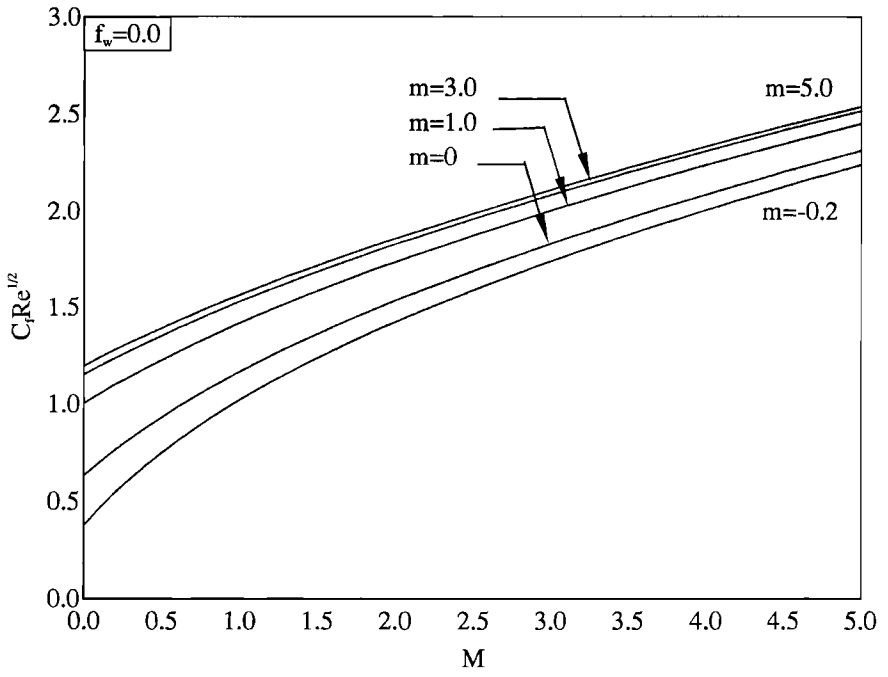

Fig. 10. Effects of M and m on skin friction coefficient.

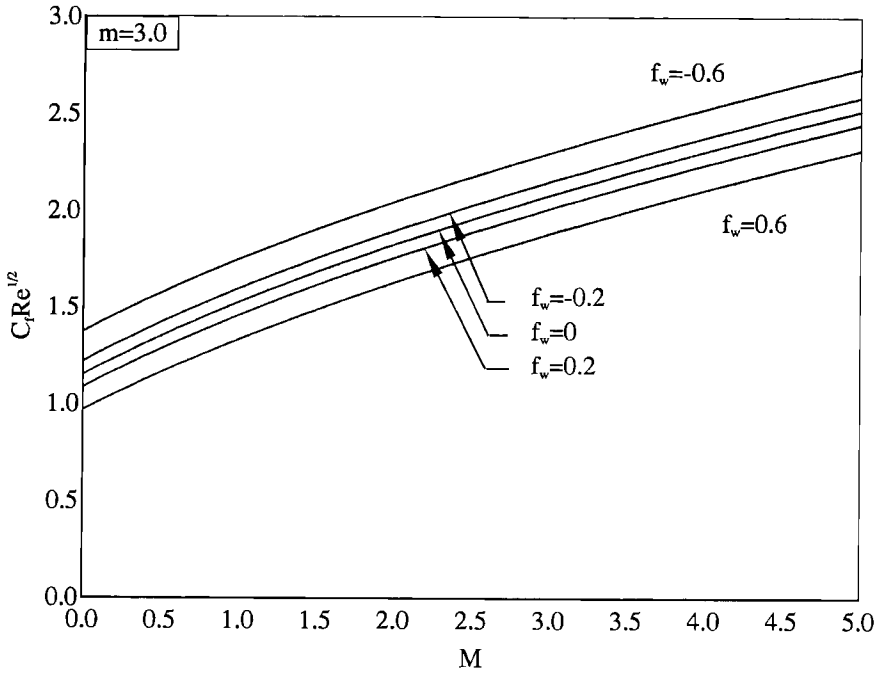

Fig. 11. Effects of M and f_w on skin-friction coefficient.

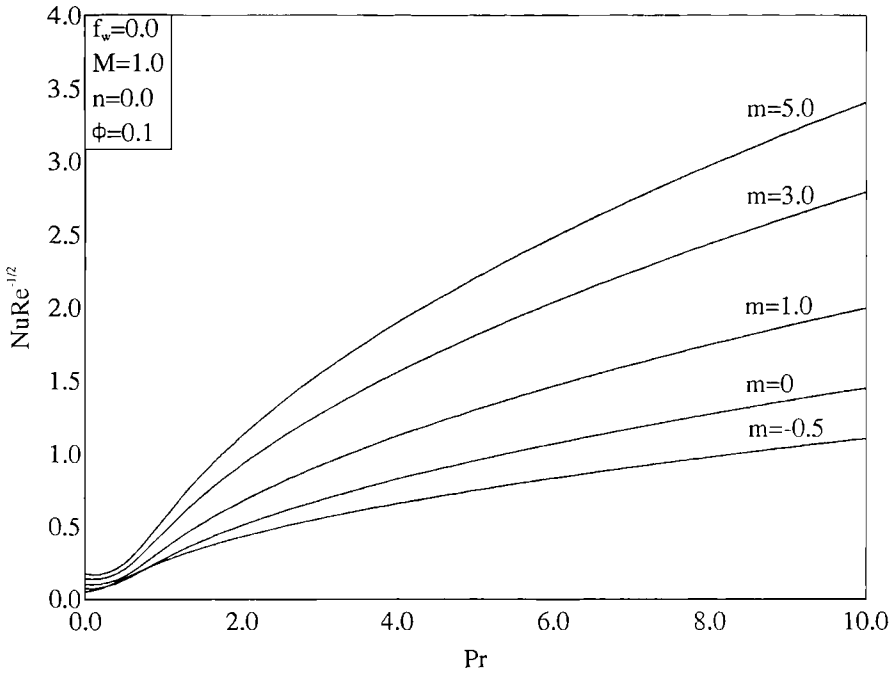

Fig. 12. Effects of Pr and m on Nusselt number.

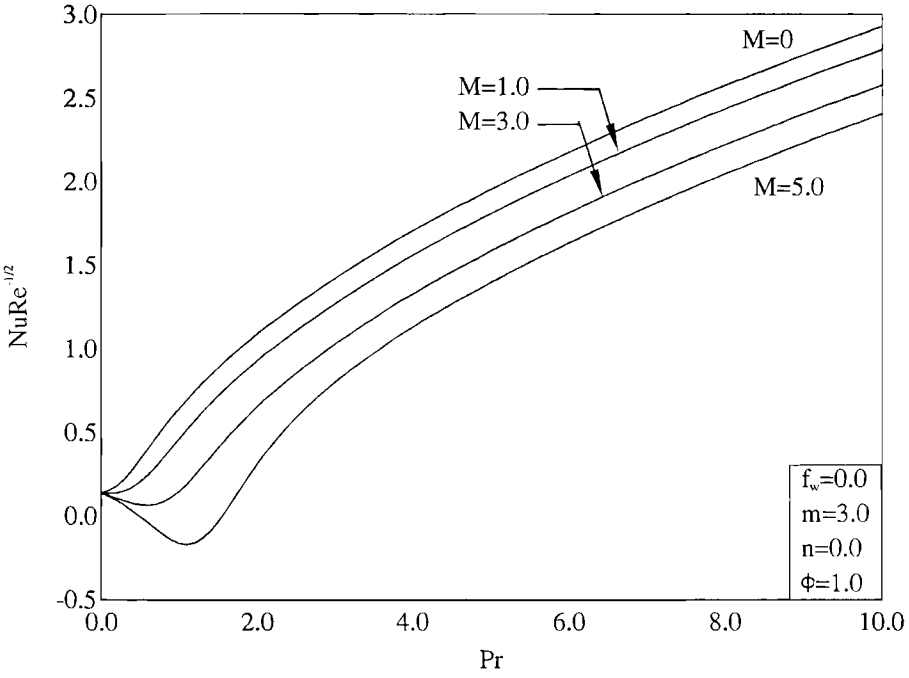

Fig. 13. Effects of Pr and M on Nusselt number.

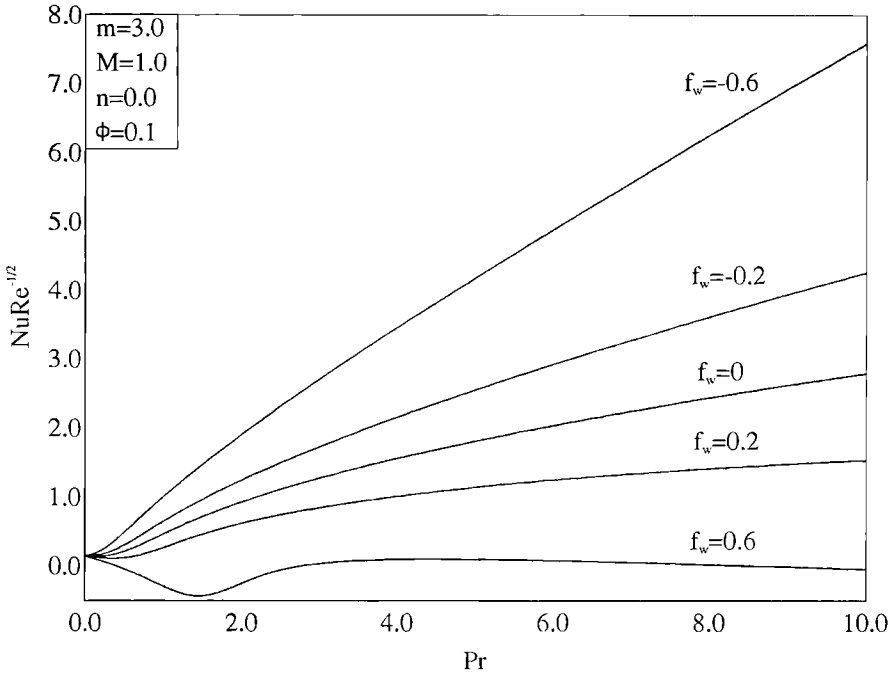

Fig. 14. Effects of Pr and f_w on Nusselt number.

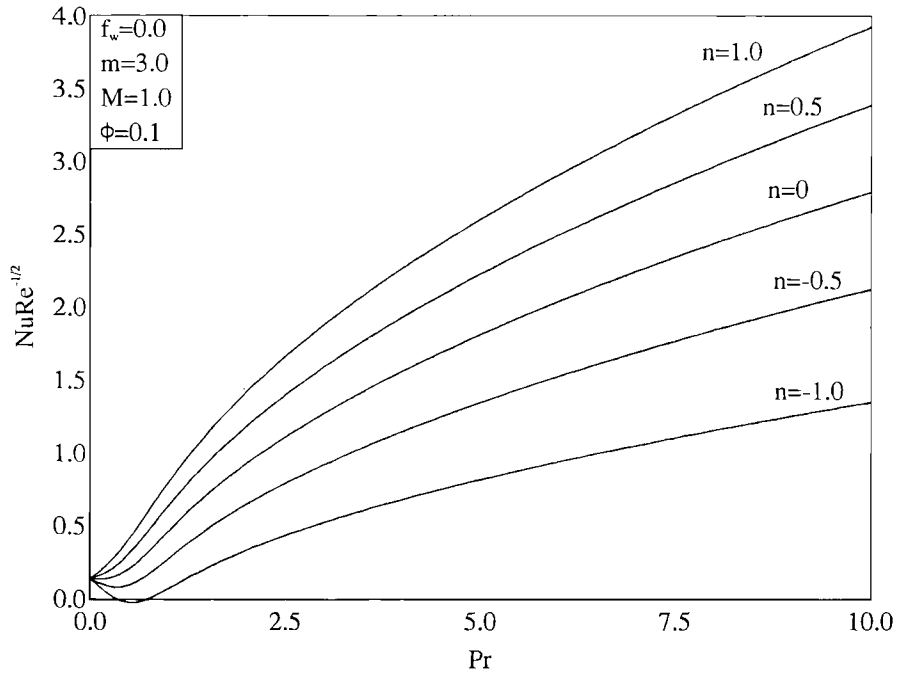

Fig. 15. Effects of Pr and n on Nusselt number.

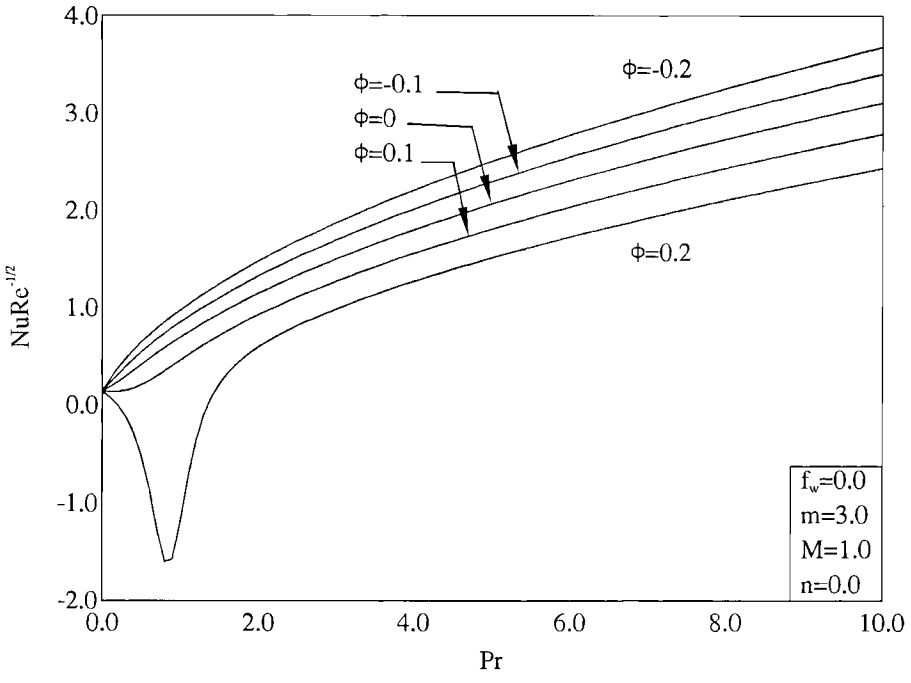

Fig. 16. Effects of Pr and ϕ on Nusselt number.

slope of the temperature profile at the wall which is directly proportional to the Nusselt number Nu, to increase. Also, it seems that, for the parametric conditions used to obtain the results, the Nusselt number increases as m increases. Furthermore, increases in either M or f_w cause the temperature gradients at the wall to decrease. This yields reductions in the values of the Nusselt number. It should be noted that for fluids with relatively low Prandtl number such as air ($\mathrm{Pr} = 0.72$), and at a high magnetic number ($M = 5$) or high wall injection velocity ($f_w = 0.6$), the Nusselt number becomes negative. This is due to the negative slopes of θ at the wall for these values. This phenomenon is evident from the temperature profiles shown in Fig. 4 and Fig. 6 in which the wall slopes change signs. All of these aspects of the Nusselt number are depicted in Fig. 12 through Fig. 14.

Fig. 15 and Fig. 16 show the Nusselt number Nu versus the Prandtl number Pr for various values of the wall temperature exponent n and the heat generation/absorption coefficient ϕ, respectively. It is clearly seen from these figures that Nu increases as n increases and decreases as ϕ increases. The sharp dip in the Nusselt number for $\phi = 0.2$ in Fig. 16 is due to the same reason discussed earlier, namely the change in the sign of the temperature slope at the wall for this case.

Conclusion

The problem of steady, laminar, incompressible, hydromagnetic boundary-layer flow and heat transfer over a power-law stretching permeable surface in the presence of a non-uniform transverse magnetic field and heat generation or absorption was formulated. The derived equations allowed for possible fluid suction or injection at the surface boundary and variable power-law surface temperature distribution. The nonlinear governing partial differential equations were transformed to ordinary differential equations by using a similarity transformation. The resulting equations were solved numerically by an implicit, iterative finite-difference method. A linearized closed-form solution for the hydrodynamic problem for large magnetic numbers was also developed. A parametric study of all the physical parameters involved in the problem was conducted and the results were illustrated graphically and discussed. Many favourable comparisons with previously published work were performed. It was found that increases in either the magnetic number or the stretching velocity exponent caused increases in the skin- friction coefficient. However, increasing the suction/injection coefficient resulted in decreasing the skin-friction coefficient. In addition, as either of the Prandtl number, the stretching velocity exponent or the wall temperature exponent was increased, the Nusselt number was increased. On the other hand, increases in either of the magnetic number, the suction/injection coefficient, or the heat generation/absorption coefficient yielded reductions in the Nusselt number. It is hoped that the present results will serve as a stimulus for experimental research dealing with the flow and thermal problem discussed in the present work.

REFERENCES

1. Afzal, N., Heat Transfer from a Stretching Surface, *Int. J. Heat Mass Transfer*, 1993, **36**, pp. 1128–1131.
2. Ali, M. E., Heat Transfer Characteristics of a Continuous Stretching Surface, *Warme-Und Stoff'ubertragung*, 1994, **29**, pp. 227–234.
3. Ali, M. E., On Thermal Boundary Layer on a Power-Law Stretched Surface with Suction or Injection, *Int. J. Heat and Fluid Flow*, 1995, **16**, pp. 280–290.
4. Ali, M. E., The Effect of Suction or Injection on the Laminar Boundary Layer development over a Stretched Surface, *J. King Saud Univ., Eng. Sci.*, 1996, No. 1, in press, 8 pages.

5. Banks, W. H. H., Similarity Solutions of the Boundary-Layer Equations for a Stretching Wall, *J. Mécanique Théorique et Appliqueé*, 1983, **2**, pp. 375–392.
6. Blottner, F. G., Finite-Difference Methods of Solution of the Boundary-Layer Equations, *AIAA J.*, 1970, **8**, pp. 193–205.
7. Chakrabarti, A. and Gupta, A. S., Hydromagnetic Flow and Heat Transfer over a Stretching Sheet, *Q. Appl. Math.*, 1979, **37**, pp. 73–78.
8. Chamkha, A. J., Non-Darcy Hydromagnetic Free Convection from a Cone and a Wedge in Porous Media, *Int. Commun. Heat Mass Transfer*, 1996, **23**, pp. 875–887.
9. Chandran, P., Sacheti, N. C., and Singh, A. K., Hydromagnetic Flow and Heat Transfer past a Continuously Moving Porous Boundary, *Int. Commun. Heat Mass Transfer*, 1996, **23**, pp. 889–898.
10. Chen, C. K. and Char, M., Heat Transfer of a Continuous Stretching Surface with Suction or Blowing, *J. Math. Anal. Appl.*, 1988, **135**, pp. 568–580.
11. Chen, T. S. and Strobel, F. A., Buoyancy Effects in Boundary Layer Adjacent to a Continuous Moving Horizontal Flat Plate, *J. Heat Transfer*, 1980, **102**, pp. 170–172.
12. Chiam, T. C., Hydromagnetic Flow over a Surface Stretching with a Power-Law Velocity, *Int. J. Eng. Sci.*, 1995, **33**, pp. 429–435.
13. Cobble, M. H., Magnetofluiddynamic Flow with a Pressure Gradient and Fluid Injection, *J. Eng. Math.*, 1977, **11**, pp. 249–256.
14. Crane, L. J., Flow past a Stretching Plane, *Z. Amgew, Math. Phys.*, 1970, **21**, pp. 645–647.
15. Erickson, L. E., Fan, L. T., and Fox, V. G., Heat and Mass Transfer on a Moving Continuous Flat Plate with Suction or Injection, *Industr. Eng. Chem.*, 1966, **5**, pp. 19–25.
16. Fox, V. G., Erickson, L. E., and Fan, L. T., Methods for Solving the Boundary Layer Equations for Moving Continuous Flat Surfaces with Suction and Injection, *AIChE J.*, 1968, **14**, pp. 726–736.
17. Grubka, L. G. and Bobba, K. M., Heat Transfer Characteristics of a Continuous Stretching Surface with Variable Temperature, *J. Heat Transfer*, 1985, **107**, pp. 248–250.
18. Gupta, P. S. and Gupta, A. S., Heat and Mass Transfer on a Stretching Sheet with Suction or Blowing, *Canad. J. Chem. Eng.*, 1977, **55**, pp. 744–746.
19. Jacobi, A. M., A Scale Analysis Approach to the Correlation of Continuous Moving Sheet (Backward Boundary Layer) Forced Convective Heat Transfer, *J. Heat Transfer*, 1993, **115**, pp. 1058–1061.
20. Lakshmisha, K. N., Venkateswaran, S., and Nath, G., Three Dimensional Unsteady Flow with Heat and Mass Transfer over a Continuous Stretching Surface, *J. Heat Transfer*, 1988, **110**, pp. 590–595.
21. Moalem, D., Steady State Heat Transfer Within Porous Medium with Temperature Dependent Heat Generation, *Int. J. Heat Mass Transfer*, 1976, **19**, pp. 529–537.
22. Sakiadis, B. C., Boundary-Layer Behavior on Continuous Solid Surfaces: I. Boundary-Layer Equations for Two-Dimensional and Axisymmetric Flow, *AIChE J.*, 1961a, **7**, pp. 26–28.
23. Sakiadis, B. C., Boundary-Layer Behavior on Continuous Solid Surfaces: II. The Boundary-Layer on a Continuous Flat Surface, *AIChE J.*, 1961b, **7**, pp. 221–225.
24. Soundalgekar, V. M. and Murty, T. V. R., Heat Transfer in MHD Flow with Pressure Gradient, Suction and Injection, *J. Eng. Math.*, 1980, **14**, pp. 155–159.
25. Soundalgekar, V. M. and Ramana Murty, T. V., Heat Transfer past a Continuous Moving Plate with Variable Temperature, *Warme-Und Stoff'ubertragung*, 1980, **14**, pp. 91–93.
26. Sparrow, E. M. and Cess, R. D., Temperature Dependent Heat Sources or Sinks in a Stagnation Point Flow, *App. Sci, Res.*, 1961, **A10**, pp. 185–197.
27. Tsou, F. K., Sparrow, E. M., and Goldstein, R. J., Flow and Heat Transfer in the Boundary

Layer on a Continuous Moving Surface, *Int. J. Heat Mass Transfer*, 1967, **10**, pp. 219–235.
28. Vajravelu, K. and Hadjinicolaou, A., Convective Heat Transfer in an Electrically Conducting Fluid at a Stretching Surface with Uniform Free Stream, *Int. J. Eng. Sci.*, 1997, **35**, pp. 1237–1244.
29. Vajravelu, K. and Nayfeh, J., Hydromagnetic Convection at a Cone and a Wedge, *Int. Commun. Heat Mass Transfer*, 1992, **19**, pp. 701–710.
30. Vleggar, J., Laminar Boundary-Layer Behavior on Continuous Accelerating Surfaces, *Chem. Eng. Sci.*, 1977, **32**, pp. 1517–1525.